en

Experimental Neurobiology

Original Article

Mesenchymal Stem Cells Improved the Ultrastructural Morphology of Cerebral Tissues after Subarachnoid Hemorrhage in Rats

Mohammad Ali Khalili[1], Fatemeh Sadeghian-Nodoushan[1,2*],
Farzaneh Fesahat[1], Seyed Mohsen Mir-Esmaeili[3,4],
Morteza Anvari[1] and Seyed Hossain Hekmati-moghadam[5]

[1]*Research and Clinical Center for Infertility, Shahid Sadoughi University of Medical Sciences, Yazd, [2]Stem Cell Biology Research Center, Shahid Sadoughi University of Medical Sciences, Yazd, [3]Yazd ACECR Higher Education Institute, Yazd, [4]Department of Biology, Faculty of Science, Sistan & Baluchestan University, Zahedan, [5]Department of Pathology, Shahid Sadoughi University of Medical Sciences, Yazd, Iran*

Subarachnoid hemorrhage (SAH) causes widespread disruption in the cerebral architecture.The process of SAH is complicated and many people lose their lives or become disabled after injury. Mesenchymal stem cells (MSCs) are considered as good candidate for repair of cerebral damage. The aim was to assess the ultrastructural changes in the rat cerebral tissue after intravenous transplantation of MSCs. Female Wistar rats (8 per group) weighing 275~300 g were assigned to control (SAH+PBS) and experimental groups (SAH+MSCs).The samples from middle cerebral arterial wall and parietal cerebral tissue were prepared for transmission electron microscopy (TEM) according to standard protocol. Fine architectures of the vessel wall, including the contraction of the inner layer, smooth muscle layer,as well as neural cells were observed after SAH. Cerebral arterial wall and cortex, including neuronal and glial cells were injured post SAH. But, administration of MSCs improved the structural integrity of cerebral tissues. Changes were much more balanced with their relative improvement in some areas. The role of MSCs for repairing the injured cerebral tissues post experimental SAH was approved by electron microscopy.

Key words: Electron microscopy, Mesenchymal stem cell, subarachnoid hemorrhage, Transplantation, rat

INTRODUCTION

Subarachnoid hemorrhage (SAH) is one of the destructive neurological diseases that lead to high mortality and disability [1]. Although the diagnosis and treatment strategies for SAH has improved and the mortality rate after SAH is decreasing, but it is still between 25~50% worldwide [2, 3]. SAH occurs in relatively young individuals, and many survivors suffer long-term neurological and cognitive disorders [4]. The aetiology and path physiology of SAH related vasospasm remain controversial [5]. Early brain injury after SAH includes cell death, inflammatory, physiological, mechanical and ionic disturbances. Inflammation occurs in the subarachnoid space, and cells such as lymphocytes and macrophages have been observed in this space 2~5 days after

initiation of SAH [6]. It has been shown that both lymphocyte-associated antigen-1 monoclonal and human anti-CD11/18 monoclonal antibodies inhibited the cerebral vasospasm after experimental SAH in the presence of hemoglobin [5]. The above data clearly showed that inflammation can play a role in formation of cerebral vasospasm after SAH. In their recent work, Rowland and colleagues (2012) reported that neurons, endothelia and astrocytes are the main cells that are damaged post SAH [6]. The constriction in arteriolesis more important than delayed vasospasm within large vessels in SAH complications [7]. It has been proposed that atrophy usually occurs in the temporal lobes after SAH that may correlate with neurocognitive deficits without any central structural lesions [8].

Mesenchymal stem cells (MSCs) have been widely used in the experimental studies, because of the proliferation and differentiation capabilities such as mesenchymal lineage cells, including neurons and cardiomyocytes, with no ethical issues [9]. These cells are capable to secret cytokines, chemokines and growth factors [10]. MSCs are recognized with great potential for cell transplantation therapy of neurological diseases and injuries to the central nervous system (CNS) [11]. Also, these cells have some advantages for autologous transplantation such as availability; easy use; the capacity to cross the blood–brain barrier, and migration throughout the CNS. In addition, MSCs enhance angiogenesis, synaptogenesis and neuritogenesis in the damaged brain tissue; they can also promote functional recovery after experimental brain injuries [12].

Transplanted MSC were shown to improve the injured area by differentiation into special region in the injection site, induction of angiogenesis, modification of inflammation, and activation of intrinsic stem or progenitor cells [10]. MSCs have been directly introduced into the injured area, or via circulation route [13]. Lately, several studies have reported the success in administration of MSCs in treating experimental stroke. However, only one study has been reported the therapeutic benefits of MSCs in experimental SAH [14]. Previously, we investigated the cerebral recovery rate with MSCs, and showed that these cells were suitable candidate for treatment of SAH in an animal model. Intravenous (I.V) transplanted MSCs were shown to differentiate into glial, neuronal, and arterial endothelial cells. Also, functional defects as end results of SAH were improved in rats receiving MSCs as measured by Neurological Severity Score (NSS) test [1]. To our knowledge, fine structure of vessel wall and cerebral cells after stem cell transplantation in SAH model has not been studied by transmission electron microscopy (TEM). Therefore, in completion of our previous work [1], the aim was to investigate the ultrastructural architecture of neural cells and cerebral arterial

wall in SAH rats receiving MSCs transplantation via I.V route.

MATERIALS AND METHODS

Sixteen female Wistar rats (8 per group) weighing 275~300 g were assigned to control (SAH+PBS) and experimental groups (SAH+MSCs).The animals were kept and cared according to the guideline of laboratory animals at our university.

### Induction of subarachnoid hemorrhage

Donor rats were anesthetized and their femoral arteries were isolated for blood withdrawal. Using a 27-guage needle, 0.3 ml of unheparinized blood was withdrawn from the donor rat and injected through the free end of the calibrated tube into the subarachnoid space of the experimental rat over 30 s. Following each injection, the tube was cleared of blood by injection of 0.05 ml of physiological saline. Rats were then given a subcutaneous injection of 1.5 mg/kg butorphanol 3 times a day on the first post operative day. The muscle layers were used to cover the tube and the wound was closed with the skin sutured around the injection tube. Each rat was placed in an individual cage and allowed to fully recover.

Animal groupings

24 h after induction of SAH, 1 ml of PBS was injected into the tail vein of rats in the control group (SAH+PBS), and 3×10^6 MSCs was administered via I.V for experimental group (SAH+MSCs). Isolation and expansion of MSCs (3 passages) was performed using tibias and femurs of male rats as bone marrow donors. The animals were killed 14 days post SAH using perfusion and fixation technique. Briefly, after induction of general anesthesia, perfusion-fixation was performed transcardially with 200 ml of 0.1 M phosphate buffer (PH 7.2, osmolarity 400~425) followed by 400 ml of 1% glutaraldehyde with 2% paraformaldehyde in 0.1 M phosphate buffer (PH 7.2). After fixation, the brains were quickly removed from the skull. Then, dorsal cortical section of parietal lobe as well as the M1 segment of middle cerebral artery (MCA), extending from its origin to where it terminates into the superior and inferior trunks was fixed in 2% paraformaldehyde for further histological assessment. The MCAs were studied primarily because of their widespread distribution to vital cortical regions.

Morphological studies

For this portion of the experiment, light microscopy was used to examine cerebral arterial wall and parietal lobe of each brain. Then, each parietal lobe was cut into seven equally spaced coronal blocks and embedded in paraffin. A series of 5 μm thick sections
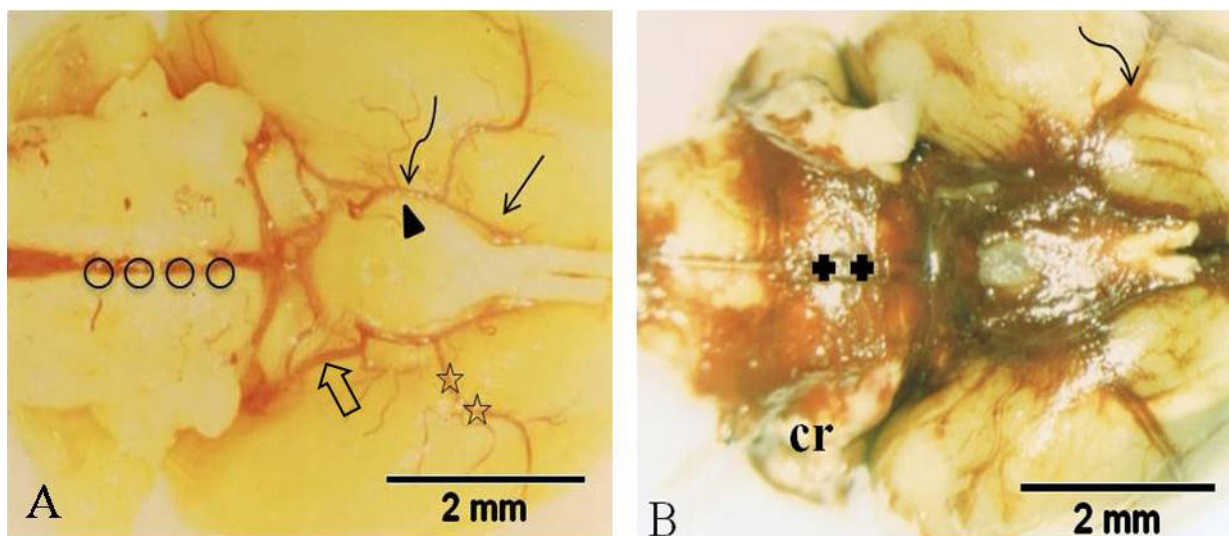
Fig. 1. Gross appearance of the circle of Willis in transcardially perfused rats. (A) The circle of Willis in normal control rat. Open circles and curved arrow mark the section of basilar artery and middle cerebral artery, respectively. Internal carotid artery (arrowheads), posterior cerebral artery (thick arrow), and anterior cerebral artery (arrow) are clearly visible. (B) The circle of Willis in post-SAH rat. Note large, organized blood clots along the lateral and ventral aspect of the medulla oblongata and basilar pons. General position of basilar artery is indicated by ++. Curved arrow indicates the position of middle cerebral artery. Cerebellum (cr).

at various levels (100 μm intervals) was cut from each block and stained with hemotoxylin and eosin (H&E) for further analysis.

Tissue processing for TEM

The specimens were washed in 0.1 M phosphate buffer, then post-fixed in 2% aqueous osmium tetroxide in 0.1 M phosphate buffer for 2 h. After several washes in deionized water, the specimens were dehydrated in a graded series of ethanol solutions. The alcohol was removed with propylene oxide, and subsequent 50/50 propylene oxide and fresh Araldite solutions (Sigma Co., USA), which was left overnight on the rotary mixer. The embedding medium was replaced twice with freshly mixed Araldite for 6 h. Each segment of tissue was embedded in fresh Araldite in individual gelatin capsules, which were finally placed in an oven for 48 h at 60°C for polymerization.

Blocks of tissue were prepared for sectioning on a Reichert Ultra microtome (OMU3). The 1 micron semi-thin sections were cut, stained with 1% Toluidine Blue in 1% sodium borate for 30 s at 60°C, and studied with light microscope. The blocks were further trimmed and 60 nm thick ultrathin sections were cut for electron microscopy. The sections were picked up on copper grids and stained with uranyl acetate for 15 min in dark and lead citrate for 2 min in a CO_2 free atmosphere. The grids were then rinsed in deionized water, dried, and stored in a grid-box. The grids were observed under a Phillips 300 TEM at accelerating voltage of 60 KV.

RESULTS

### General and gross examination

The SAH rats developed drowsiness, but none of them showed any severe paralysis. Clot accumulation was observed over the ventral surface of the brains. The clot accumulation usually extended from the medulla to the superior border of the pons in contact with basilar arteries. Clots were similarly scattered in areas around the origin of middle cerebral arteries (Fig. 1).

The cerebral vasculatures as well as cerebral tissue from parietal lobe of animals that underwent MSC therapy did not show any noticeable changes at light microscopy level, when compared with the rats from the other group (Fig. 2, 3). Mild spasms were observed in some cerebral arteries. In addition, cellular infiltration was observed in cerebral tissues from experimental animals (Fig. 3B).

Control group (SAH+PBS)

Arterial layers of intima, media, and adventitia showed severe abnormalities in rats sacrificed post SAH (Fig. 4A, C). The intimal surface of the MCA showed structural evidence of contraction. Smooth muscle necrosis with numerous vacuoles filled with amorphous material and degenerating mitochondria were other arterial alterations (4A). The myo-necrosis with disruption of myofibrillar structure or cellular membranes and increased amount of material (i.e. collagen) in the intercellular spaces
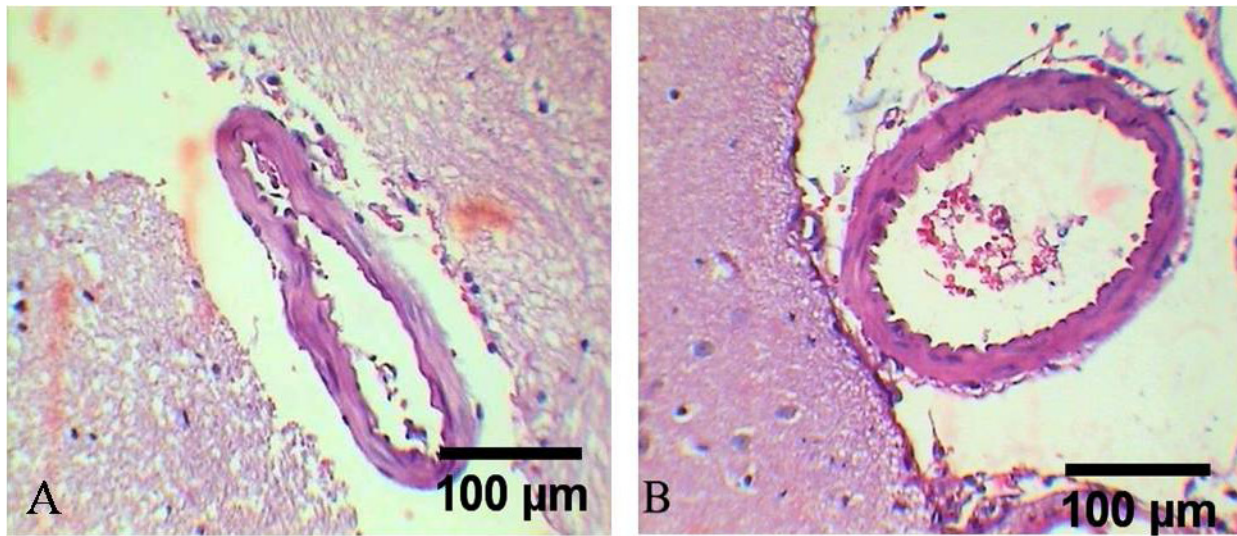
Fig. 2. Light micrograph of middle cerebral artery from experimental groups. (A) Note the absence of spasm or heavy corrugation in SAH+PBS rat. (B) A severely spastic middle cerebral artery from a rat in SAH+MSC group.
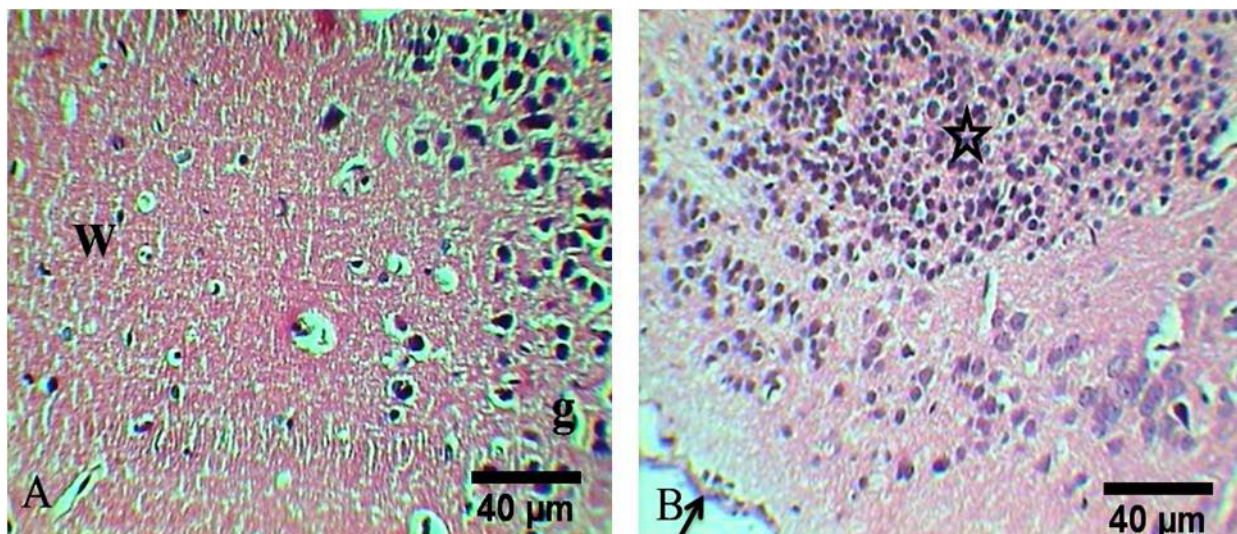

Fig. 3. Cerebral tissue of parietal lobe from rats. (A) The section showing the general appearance of the gray (g) and white (w) matters in SAH+PBS rat. Extensive neural swellings are visible in cortex. (B) Part of cerebral tissue in SAH+MSC group. Note the heavy infiltration of cerebral cellular elements (star). Arrow indicates the surface of parietal lobe.

contributed to medial thickening of the arterial wall (Fig. 4A). In addition, varying degrees of cortical injury, including the presence of injured dark neuron surrounded by few normal neuronal cells, were observed in cortex following SAH (Fig. 5A, 6A). Electron microscopy showed swelling of numerous neuronal mitochondria. Also, considerable extracellular edema was observed in the cortical sections (6A). In addition, axonal degeneration with ruffling of the laminae of the myelin sheaths was other ultrastructural findings (Fig. 6A). Presence of degenerated dark neurons with amorphous appearance of cytoplasm were other findings in SAH+PBS rats

(Fig. 6C). Fine morphological status in cerebral tissues of rats summarized in Table 1.

Experimental group (SAH+MSC)

The ultrastructure of the arterial wall was relatively uninterrupted, with no area devoid of endothelial cells (Fig. 4 B). However, convoluted endothelia were clearly visible (Fig. 4D). Four to five layers of smooth muscle cells with no muscle necrosis were apparent (Fig. 4B). In some areas, intercellular irregularity was noticeable. Also, there were no adventitial inflammatory
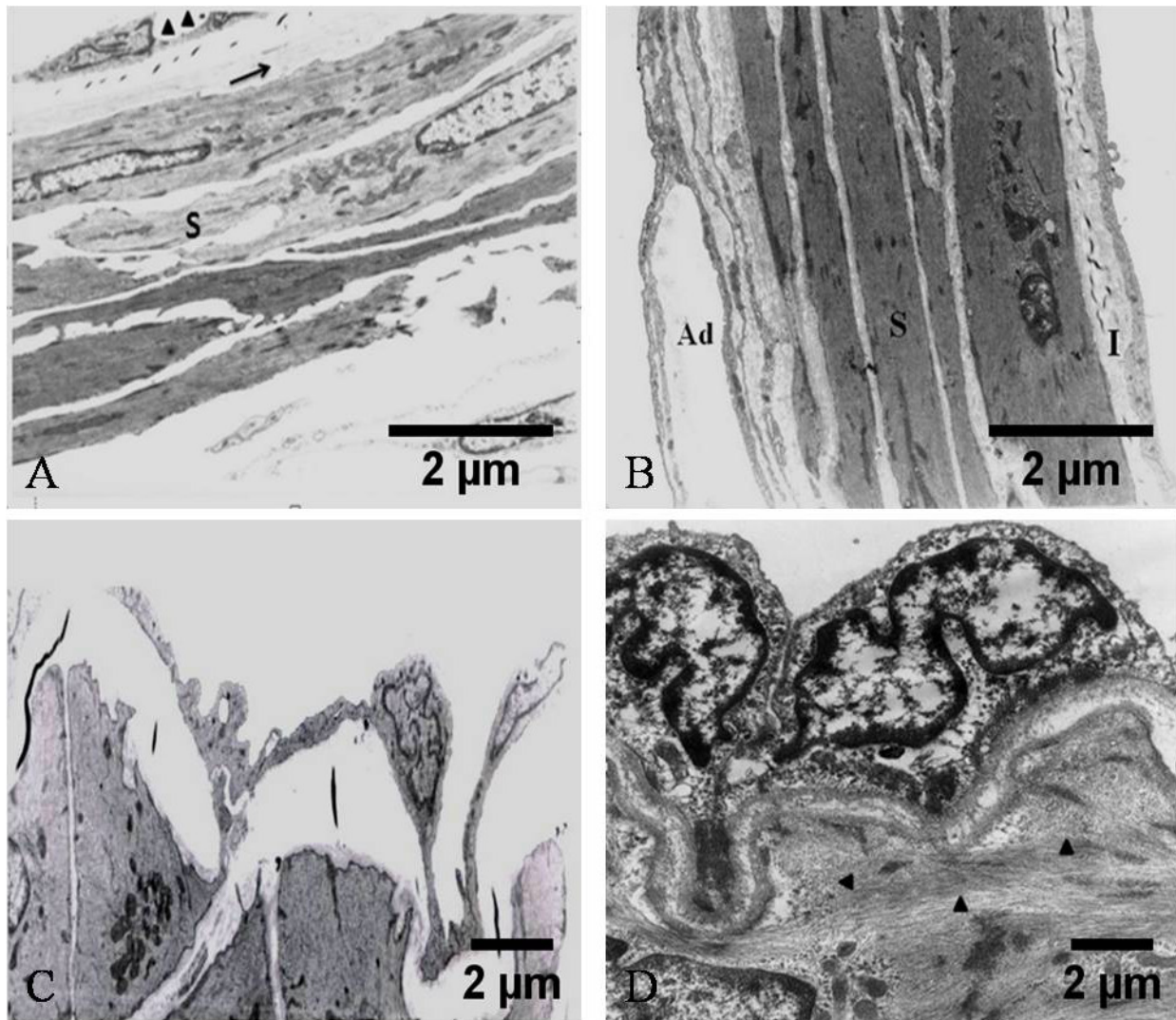
Fig. 4. Ultrastructure of middle cerebral arteries from animals in different groups. (A) Convoluted and distorted endothelial cells (arrowheads). Note, severely injured smooth muscle cell (s) with irregularly widened intercellular spaces are demonstrated in artery from group SAH+PBS. Sub endothelial cell debris (arrow). (B) Entire arterial wall following SAH+MSC. Mild injury to all layers (intima, media, and adventitia) is visible. Internal elastic membrane (I); smooth muscle cell (S); adventitial layer (ad). (C) The irregular surface of the luminal side after SAH+PBS. Convoluted endothelial cells with severely invaginated nuclei are visible. (D) Noticeable convoluted and distorted endothelial cells, migration of cellular debris into the widened subintimal layer (arrowheads) are clearly demonstrated in spastic arterial wall in group SAH+MSC.

infiltrates (Fig. 4B). The fine picture of neural tissue revealed intact neurons with well-defined nuclear membrane (Fig. 5B). However, some dendritic damages were noticed in some neural area (Fig. 6D). The Golgi apparatus and mitochondria showed no unusual features, and were distributed normally in the cell body (Fig. 6B, D, and E). In brief, the nucleoli, nucleus, Nissl substance, and cellular organelles were not altered. In addition, there was no sign of edema in the parietal cortex (Fig. 6D, E). Table 1 presents the ultra-morphological status in cerebral tissues of SAH+MSC rats.

DISCUSSION

Electron microscopic study of cerebral sections showed that both blood vessels and cerebral tissue were altered after SAH. In previous studies, electron microscopy was used to describe ultrastructural differences in great arteries surrounding the area of hemorrhage [15-18]. These observations were accompanied by vasoconstriction and pathological changes as endothelial cell swelling, internal elastic lamina thickening, endothelial and smooth muscle cell vacuolation and necrosis and loss of inter endothelial cell tight junctions [19-21]. Also, Micro-vessel constriction and
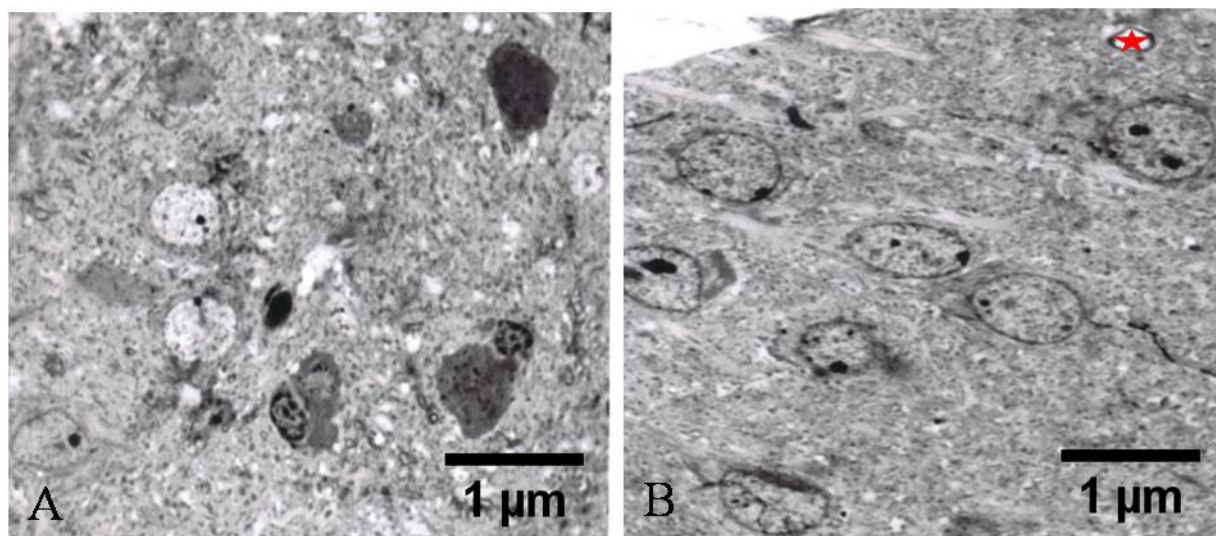
Fig. 5. Semi-thin sections of parietal corteses. (A) Few injured neurons "dark neurons" surrounded by normal neurons from semi-thin of SAH+PBS rat. (B) Normal neuronal cells from animal in SAH+MSC group. Note intact neurons with large nuclei and prominent nucleoli. Cortical capillary (star).

reduced blood flow were observed with video microscopic system within 2 h of SAH in rats [22]. In another study; arterioles were damaged by microthrombi in SAH mice which showed higher rates of arteriole constriction when compared with the control group [23].

Mecklenburg and colleagues noticed ultra structural changes in the cerebral arteries in triple cisternal blood injection model in the baboon 7 days after the stimulation of SAH. The muscular layers started to destroy and the inter cellular space collagens were increased. In addition, the endothelial layers were disrupted and their tight junctions were lost [24]. However, Pickard et al. [25] did not observe any ultra structural changes within the cerebral arteries up to nine days after SAH in dogs. They, however, noticed the presence of some white blood cells and macrophages in the subarachnoid space and debris left by the SAH. In other studies, platelet adhesion and embolic materials were seen; but, ultrastructural differences in the micro-vessels and parenchymal vessels after SAH were not observed [23]. The ultrastructural disorders in arteries were associated with hypertension, atherogenesis, and endothelial damage after SAH [26]. Similar changes were also observed in our arterial findings, such as, vascular contraction, endothelial injury, and smooth muscle disruption. Also, intercellular spaces, cortical cellular microanatomy and nerve fibers had noticeably changed in SAH animals. Another finding in cerebral cortex of rats after induction of SAH was the presence of degenerated neurons, known as "dark neurons" surrounded by normal neuronal cells. These cells represent a neuronal injury, however reversible, after hypoglycemia [27]. Furthermore, the presence of macrophages

in association with injured cortical sections indicated the phagocytosis of cellular debris was in progress. These observations further suggest that the neuronal response to diffuse impaired circulation would vary, where some neural components would be injured- dark neuron, others would be morphologically intact. Also, Giulian and Vaca (1993) suggested that brain inflammatory cells, blood-borne macrophages, during their phagocytic activities are the source of free radicals that participate in contact-mediated killing of neuronal cells, creating dark neurons. Also, the cytotoxic molecules released by injured or dying neural tissues are likely to be responsible for delayed ischemia [28].

The basilar artery changes were studied with both TEM and angiography 3~7 after SAH in dogs [29]. More severe vasospasm was associated with a reduction in the diameter of arteries from 3~7 days. Apoptotic-like changes were also observed in endothelial cells with cytoplasm and nuclear chromatin condensation around cortical and neurons that were damaged post cerebral ischemic stroke [29]. Ultra structural alterations in cortical neurons were inflated cytoplasm, abnormal organelles, vacuole formation and damaged membrane. However, both apoptotic and necrotic characteristics were evident in thalamic neurons. The nuclear shrinkage, chromatin condenses and cytoplasmic changes were observed as mentioned above [30].

The changes in neural stem cells (NSCs) can be traced with electron microscopic studies in animal models. Neurons derived from transplanted NSCs creating synaptic contacts are appropriate for use in the treatment of human vascular Parkinsonism [31]. Also, TEM assessment showed that NSCs can integrate into the host brain and are associated with neuronal differentiation [32, 33].
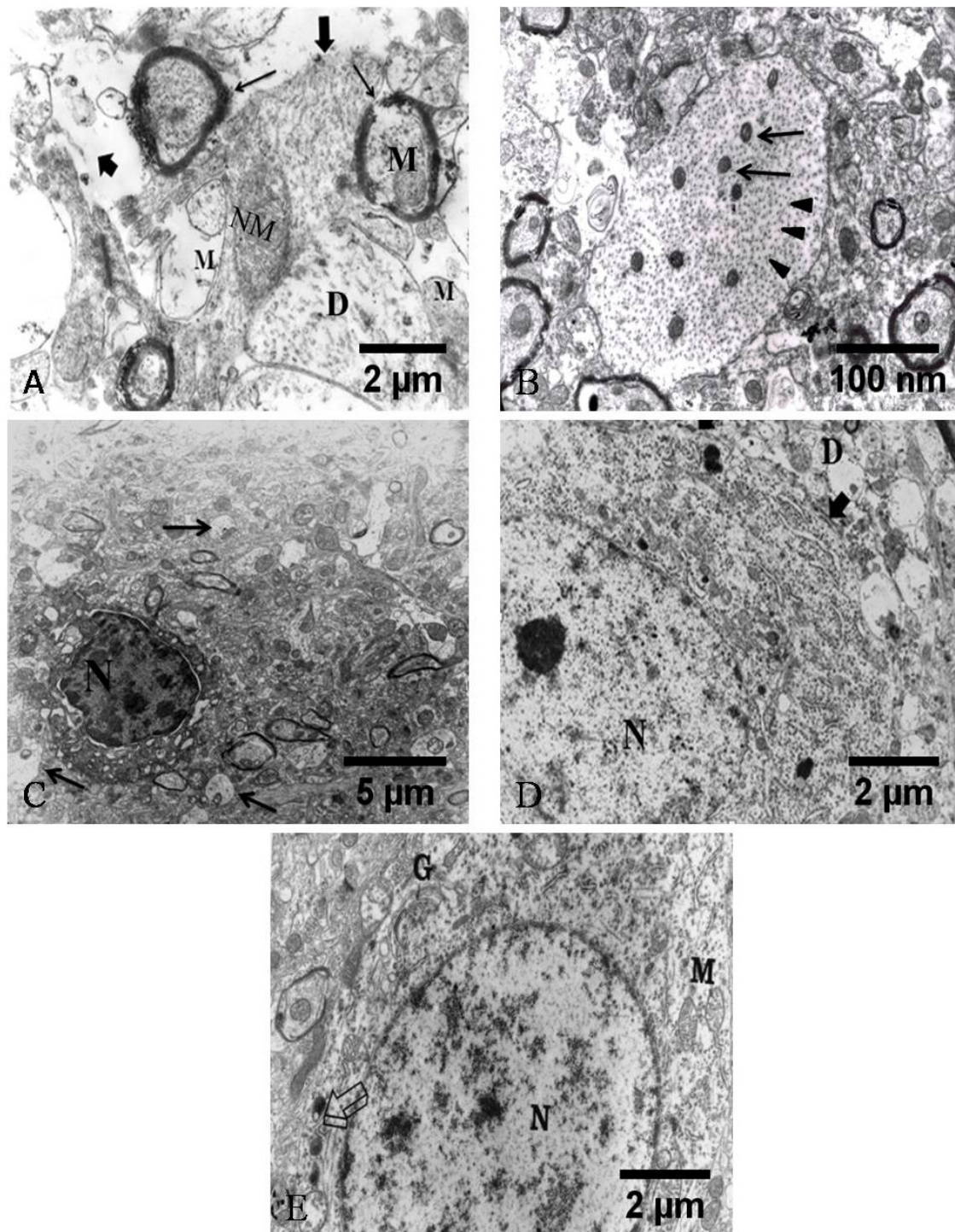
Fig. 6. Ultrastructual images of parietal corteses in different rat groups. (A) Damaged neural elements, including myelinated axon (arrow) from SAH+PBS. Note the pre-neural edema (solid arrow) and degenerated mitochondrion (M) in vicinity of normal mitochondrion (NM). Also, the dendrite (D) is abnormally shaped and distorted. (B) In the center of the field is a large transversally sectioned dendrite from SAH+MSC rat. Evenly spaced microtubules (arrow) are scattered in the dendritic cytoplasm. Arrowheads indicate the neurofilaments. There are also several relatively damaged myelinated axons with normal mitochondria. (C) An injured neuron "dark neuron" with characteristic of cell death, including the amorphous appearance of the cytoplasm, and disappearance of the nuclear membrane from SAH+PBS group. Damaged neural elements (arrows) are shown in this micrograph. Nucleus (N). (D) A relatively normal neuron with a prominent nucleolus and number of axon terminals (solid arrow) synapse with the cell body of the neuron from SAH+MSC group. Note, also the denderites (D) with no sign of damage. Nucleus (N). (E) Much of the perikaryon is occupied by a large round nucleus (N) in SAH+MSC group. Note the presence of lipofuscin bodies (arrow) within the cytoplasm. Golgi apparatus (G); mitochondria (M).

Table 1. Summary of the morphological status in cerebral tissues in different groups of rats

TEM observation	SAH+PBS	SAH+MSC
Endothelium		
Convoluted	+	+
Invaginated nucleus	+	+
Distortion	+	+
Sub endothelium		
Debris	+	+
Muscular layer		
Necrosis	+	-
Intercellular irregularity	+	+
Cerebral tissue		
Neuronal degeneration	+	--
Damaged axon	+	+
Dendrite distortion	+	-
Pre-neural edema	+	-
Degenerated mitochondrion	+	-

It is not yet fully clear that which mechanism occurs post MSCs injection to help injured cerebral tissue. Others reported that migration of MSCs towards damaged brain tissue depends on the specific signals expressed in astrocytes, neurons, and endothelial cells [34]. It seems that MSCs stimulate the cerebral area to activate endogenous restorative and regenerative mechanisms [35]. There is also some evidence indicating that stem cells have some kinds of intrinsic capacity to detect pathological areas within the brain, such as VEGF factors that are released in many neurological disorders. These vital growth factors can migrate towards damaged cerebral areas or traumatized brain [36]. Also, MSCs in TBI rats were shown to increase the number of microglia/macrophages in the injured area, particularly in the lumen near the lesion. These cells are able to produce several neurotrophic factors, which may activate endogenous repair processes in the damaged brain [12]. We were unable to find any related studies examining the electron microscopic changes within cerebral tissues after MSC transplantation in an animal model. Our TEM images confirmed that introduction of stem cells were involved in the fine recovery of the affected areas. In most regions, undisturbed neurons with distinct nuclear membrane as well as arterial wall repair were observed. There was less variation accompanied by partial improvement in SAH group after MSC transplantation, which is consistent with our previous observation [1]. In Conclusions, TEM observations confirmed that MSCs were capable of improving the damaged areas within cerebral tissues post SAH in rat. Further studies may confirm the possible applicability of MSCs in SAH therapy.

REFERENCES

1. Khalili MA, Anvari M, Hekmati-Moghadam SH, Sadeghian-Nodoushan F, Fesahat F, Miresmaeili SM (2012) Therapeutic benefit of intravenous transplantation of mesenchymal stem cells after experimental subarachnoid hemorrhage in rats. J Stroke Cerebrovasc Dis 21:445-451.

2. Nieuwkamp DJ, Setz LE, Algra A, Linn FH, de Rooij NK, Rinkel GJ (2009) Changes in case fatality of aneurysmal subarachnoid haemorrhage over time, according to age, sex, and region: a meta-analysis. Lancet Neurol 8:635-642.

3. Al-Khindi T, Macdonald RL, Schweizer TA (2010) Cognitive and functional outcome after aneurysmal subarachnoid hemorrhage. Stroke 41:e519-e536.

4. Macdonald RL, Higashida RT, Keller E, Mayer SA, Molyneux A, Raabe A, Vajkoczy P, Wanke I, Bach D, Frey A, Marr A, Roux S, Kassell N (2011) Clazosentan, an endothelin receptor antagonist, in patients with aneurysmal subarachnoid haemorrhage undergoing surgical clipping: a randomised, double-blind, placebo-controlled phase 3 trial (CONSCIOUS-2). Lancet Neurol 10:618-625.

5. Xin ZL, Wu XK, Xu JR, Li X (2010) Arachnoid cell involvement in the mechanism of coagulation-initiated inflammation in the subarachnoid space after subarachnoid hemorrhage. J Zhejiang Univ Sci B 11:516-523.

6. Rowland MJ, Hadjipavlou G, Kelly M, Westbrook J, Pattinson KT (2012) Delayed cerebral ischaemia after subarachnoid haemorrhage: looking beyond vasospasm. Br J Anaesth 109:315-329.

7. Tso MK, Macdonald RL (2013) Acute Microvascular Changes after Subarachnoid Hemorrhage and Transient Global Cerebral Ischemia (in press).

8. Han SM, Wan H, Kudo G, Foltz WD, Vines DC, Green DE, Zoerle T, Tariq A, Brathwaite S, DAbbondanza J, Ai J, Macdonald RL (2013) Molecular alterations in the hippocampus after experimental subarachnoid hemorrhage. J Cereb Blood Flow Metab 34:108-117.

9. Patel AN, Genovese J (2011) Potential clinical applications of adult human mesenchymal stem cell (Prochymal°) therapy. Stem Cells Cloning 4:61-72.

10. Gala K, Burdzińska A, Idziak M, Makula J, Pączek L (2011) Characterization of bone-marrow-derived rat mesenchymal stem cells depending on donor age. Cell Biol Int 35:1055-1062.

11. Prabhakaran MP, Venugopal JR, Ramakrishna S (2009) Mesenchymal stem cell differentiation to neuronal cells on electrospun nanofibrous substrates for nerve tissue

engineering. Biomaterials 30:4996-5003.

12. Opydo-Chanek M, Dąbrowski Z (2011) Response of astrocytes and microglia/macrophages to brain injury after bone marrow stromal cell transplantation: a quantitative study. Neurosci Lett 487:163-168.

13. Choong PF, Mok PL, Cheong SK, Leong CF, Then KY (2007) Generating neuron-like cells from BM-derived mesenchymal stromal cells in vitro. Cytotherapy 9:170-183.

14. Dharmasaroja P (2009) Bone marrow-derived mesenchymal stem cells for the treatment of ischemic stroke. J Clin Neurosci 16:12-20.

15. Varsos VG, Liszczak TM, Han DH, Kistler JP, Vielma J, Black PM, Heros RC, Zervas NT (1983) Delayed cerebral vasospasm is not reversible by aminophylline, nifedipine, or papaverine in a "two-hemorrhage" canine model. J Neurosurg 58:11-17.

16. Liszczak TM, Varsos VG, Black PM, Kistler JP, Zervas NT (1983) Cerebral arterial constriction after experimental subarachnoid hemorrhage is associated with blood components within the arterial wall. J Neurosurg 58:18-26.

17. Tanabe Y, Sakata K, Yamada H, Ito T, Takada M (1978) Cerebral vasospasm and ultrastructural changes in cerebral arterial wall. An experimental study. J Neurosurg 49:229-238.

18. Tani E, Yamagata S, Maeda Y, Ito Y (1978) Cytochemical demonstration of adenylate and guanylate cyclases in vascular smooth muscle of circle of Willis. J Neurosurg 49:239-248.

19. Findlay JM, Weir BK, Kanamaru K, Espinosa F (1989) Arterial wall changes in cerebral vasospasm. Neurosurgery 25:736-745.

20. Khalili MA, Clower B (1994) 19 Pathogenesis of cerebral vasospasm following experimental subarachnoid haemorrhage in rat - a double haemorrhage model. J Anat 185:210-211.

21. Khalili MA, Clower BR (2001) Correlation between endothelial injury and cerebral vasospasm following a double subarachnoid hemorrhage in the rat. Med J Islam Repub Iran 15:93-101.

22. Sun BL, Zheng CB, Yang MF, Yuan H, Zhang SM, Wang LX (2009) Dynamic alterations of cerebral pial microcirculation during experimental subarachnoid hemorrhage. Cell Mol Neurobiol 29:235-241.

23. Sabri M, Ai J, Lakovic K, D'Abbondanza J, Ilodigwe D, Macdonald RL (2012) Mechanisms of microthrombi formation after experimental subarachnoid hemorrhage. Neuroscience 224:26-37.

24. von Mecklenburg C, Chang JY, Delgado T, Owman C, Sahlin C, Svendgaard NA (1990) Ultrastructural cerebrovascular changes in a model of subarachnoid hemorrhage in baboon based on triple cisternal blood injection. Surg Neurol 33:195-201.

25. Pickard JD, Graham DI, Matear E, MacPherson P, Tamura A, Fitch W (1985) Ultrastructure of cerebral arteries following experimental subarachnoid haemorrhage. J Neurol Neurosurg Psychiatry 48:256-262.

26. Mayberg MR, Okada T, Bark DH (1990) The significance of morphological changes in cerebral arteries after subarachnoid hemorrhage. J Neurosurg 72:626-633.

27. Auer RN, Kalimo H, Olsson Y, Siesjö BK (1985) The temporal evolution of hypoglycemic brain damage. I. Light- and electron-microscopic findings in the rat cerebral cortex. Acta Neuropathol 67:13-24.

28. Giulian D, Vaca K (1993) Inflammatory glia mediate delayed neuronal damage after ischemia in the central nervous system. Stroke 24:I84-I90.

29. Zubkov AY, Tibbs RE, Clower B, Ogihara K, Aoki K, Zhang JH (2002) Morphological changes of cerebral arteries in a canine double hemorrhage model. Neurosci Lett 326:137-141.

30. Wei L, Keogh CL, Whitaker VR, Theus MH, Yu SP (2005) Angiogenesis and stem cell transplantation as potential treatments of cerebral ischemic stroke. Pathophysiology 12:47-62.

31. Muñetón-Gómez VC, Doncel-Pérez E, Fernandez AP, Serrano J, Pozo-Rodrigálvarez A, Vellosillo-Huerta L, Taylor JS, Cardona-Gómez GP, Nieto-Sampedro M, Martínez-Murillo R (2012) Neural differentiation of transplanted neural stem cells in a rat model of striatal lacunar infarction: light and electron microscopic observations. Front Cell Neurosci 6:30.

32. Banerjee S, Williamson DA, Habib N, Chataway J (2012) The potential benefit of stem cell therapy after stroke: an update. Vasc Health Risk Manag 8:569-580.

33. Daadi MM, Li Z, Arac A, Grueter BA, Sofilos M, Malenka RC, Wu JC, Steinberg GK (2009) Molecular and magnetic resonance imaging of human embryonic stem cell-derived neural stem cell grafts in ischemic rat brain. Mol Ther 17:1282-1291.

34. Li Y, Chopp M (2009) Marrow stromal cell transplantation in stroke and traumatic brain injury. Neurosci Lett 456:120-123.

35. Chopp M, Li Y (2002) Treatment of neural injury with marrow stromal cells. Lancet Neurol 1:92-100.

36. Collins RT (2013) Neural stem cells reach gliomas intranasally. Neurol Today 13:1,4-5.